Available online at www.sciencedirect.com

ScienceDirect

Journal of the European Ceramic Society 27 (2007) 1791–1796

www.elsevier.com/locate/jeurceramsoc

Microstructural study of opaque glazes obtained from frits of the system: SiO_2-Al_2O_3-B_2O_3-(P_2O_5)-CaO-K_2O-TiO_2

Encarna Bou [*], Arnaldo Moreno, Agustín Escardino, Ana Gozalbo

Instituto de Tecnología Cerámica, Asociación de Investigación de las Industrias Cerámicas,
Universitat Jaume I, Campus Universitario Riu Sec, Castellón, Spain

Abstract

Opaque ceramic tile glazes can be obtained by using a type of frit based on the system SiO_2-Al_2O_3-B_2O_3-CaO-K_2O-TiO_2. In these glazes, opacification and whiteness are due to the presence of titanite (sphene) crystals, formed by devitrification during firing from the frit applied in the form of a glaze composition onto the ceramic body. Though not widely used in tile manufacture, this type of frit is considered an alternative to the zirconium-containing frits currently used for fabricating opaque ceramic glazes.

The present study shows that the addition of small quantities (around 1%, w/w) of P_2O_5 to a frit composition of the above oxide system considerably modifies resulting glaze gloss, converting a matt glaze into a glossy glaze.

In order to determine how the P_2O_5 addition contributes to increasing gloss in opaque white wall tile glazes, we determined the arising changes in glaze melt viscosity and glaze microstructure, establishing the latter by scanning electron microscopy (SEM) and X-ray diffraction (XRD). The results show that the presence of P_2O_5 inhibits wollastonite devitrification in the glaze melt and gives rise to changes in sphene crystal morphology, modifying glaze microstructure.

Keywords: Microstructure-final; Colour; Traditional ceramics; Opaque glazes

1. Introduction

Glossy opaque white glazes are typically obtained in ceramic wall tile manufacture from glaze compositions prepared with frits containing ZrO_2. In this type of glaze, opacification and whiteness are due to zircon devitrification from the frit during tile firing.[1–3]

Large price swings in the raw material used to contribute ZrO_2 (as zircon flour) to the frit[4–7] have driven the search for new frit compositions without ZrO_2, which yield glossy opaque white glazes. One such type of frit is based on the system SiO_2-Al_2O_3-B_2O_3-CaO-K_2O-TiO_2. In this case, the resulting opacification and whiteness are due to the presence of titanite (sphene) $CaO\cdot TiO_2\cdot SiO_2$ crystals, which devitrify from the frit in the glaze composition during tile firing.[8,9]

Previous studies[10] have shown that although compositions based on this system tend to generate opaque white glazes, such glazes display low gloss compared with the gloss typically obtained with frits containing ZrO_2. Gloss could be increased in these glazes by using Na_2O instead of K_2O in frit preparation; however, this raises glaze fusibility at low temperatures, which makes using Na_2O unfeasible in single-fired wall tile manufacture. The alternative subsequently found for raising glaze gloss has involved adding small amounts of phosphorus pentoxide (P_2O_5) to the frit composition.[10]

The present study has been undertaken to determine how the P_2O_5 addition contributes to increasing gloss in opaque white wall tile glazes. For this, we first determined the evolution of glaze aesthetic characteristics as a function of frit P_2O_5 content, establishing the optimum P_2O_5 addition that would yield a glaze with acceptable aesthetic characteristics. This frit composition was then used to study the effect of the P_2O_5 addition on glaze microstructure, and on the evolution of the crystalline phases in the resulting glazes.

2. Experimental procedure

The study was conducted using a starting frit composition, referenced T, consisting of: 64.0% SiO_2, 4.6% Al_2O_3, 5.0% B_2O_3, 13.9% CaO, 5.9% K_2O and 6.5% TiO_2. Progressive

---

[*] Corresponding author. Tel.: +34 964342424; fax: +34 964342425.
E-mail address: ebou@itc.uji.es (E. Bou).

0955-2219/$ – see front matter © 2006 Elsevier Ltd. All rights reserved.
doi:10.1016/j.jeurceramsoc.2006.04.148

additions of P_2O_5 were made to this composition. This yielded test compositions TP05, TP1, TP2 and TP3, which, respectively, contained 0.5, 1.0, 2.0 and 3.0% P_2O_5. The subsequent microstructural characterisation was only conducted on compositions T and TP1.

2.1. *Glaze preparation*

A frit was prepared from each test composition by fusing the raw materials in an electric kiln at a maximum temperature of 1500 °C, with a 30-min soak at this temperature, followed by quenching in water at ambient temperature to obtain the frit.

The resulting frit was used to prepare a glaze, whose solid content comprised 92% frit and 8% kaolin (both percentages by weight), and the necessary additives (binder and deflocculant) for wet application.

Each glaze composition was then applied onto a previously fired ceramic body, coated with a suitable engobe. The glazed pieces were fired in an electric laboratory kiln, using a thermal cycle with a constant heating rate (25 °C/min) up to a peak temperature of 1100 °C, followed by 6-min isothermal treatment at this temperature.

Certain characterisation tests required having the glazes in powder form. For these tests, the relevant glaze suspensions were dried to obtain the corresponding powder.

2.2. *Characterisation techniques*

The chromatic coordinates of the glaze coatings were determined with a spectrophotometer that performs the measurements according to the CIELab system, using a C illuminant and 2° standard observer. Gloss was determined with a reflectometer at a 60° angle of incidence.

Surface roughness was determined with an optical profilometer, using white-light interferometry. The resulting topographies were used to obtain Ra (the arithmetic mean of the absolute values of the distance of the points that compose the profile to a mean line), which is the most representative parameter of mean surface roughness.

Glaze behaviour under heat treatment was studied with a hot stage microscope, using glazes in powder form. The following characteristic temperatures were determined: T_{IC} (shrinkage start), T_{FC} (shrinkage end), T_R (softening), T_E (sphere), $T_{1/2}$ (half-sphere) and T_F (melting).

Differential thermal analysis (DTA) was run to determine the temperatures at which microstructural changes occurred. These tests were performed on glaze samples in powder form in air atmosphere with α-Al_2O_3 liners, using a heating rate of 10 °C/min.

Table 2
Characteristic temperatures of frits T (without P_2O_5) and TP1 (with 1 wt% P_2O_5)

Characteristic temperatures (°C)	T	TP1
Shrinkage start (T_{IC})	830 ± 10	830 ± 10
Shrinkage end (T_{FC})	970 ± 10	980 ± 10
Softening (T_R)	1140 ± 15	1150 ± 15
Sphere (T_E)	1160 ± 20	1160 ± 20
Semi-sphere ($T_{1/2}$)	1210 ± 20	1230 ± 20
Melting (T_F)	1240 ± 20	1250 ± 20

We characterised the glazes microstructurally with a scanning electron microscope (SEM) fitted with an energy-dispersive X-ray (EDX) microanalysis system. The proper surfaces and/or cross sections of the glazed test specimens were thus observed and analysed. To observe the cross sections, the glazed pieces were embedded in resin and then polished.

The crystalline structures in the glazes were identified by X-ray diffraction (XRD). To determine the phases present at a given firing temperature, we prepared samples of the glazes in powder. These were subjected to the same thermal cycle as the one indicated in the preparation of the glazed pieces, only modifying the isothermal treatment temperature.

3. Results

3.1. *Effect of the P_2O_5 addition on glaze aesthetic properties*

The results of the determination of fired glaze aesthetic characteristics (colour and gloss) and surface roughness are set out in Table 1. The table shows that the addition of small amounts of P_2O_5 to frit T raises gloss considerably, owing to the decrease in surface roughness. However, whiteness diminishes as frit P_2O_5 content increases.

The table shows that adding 1 wt% P_2O_5 yields a glaze with high gloss, and acceptable opacity and whiteness. The remainder of the study therefore focused on compositions T and TP1.

Glaze surface roughness can alter, owing to a variation in glaze melt viscosity or in glaze microstructure. In order to verify whether the P_2O_5 addition to frit T altered melt viscosity, fusion tests were conducted in a hot stage microscope with frits T and TP1. The characteristic temperature data obtained are detailed in Table 2.

It can be observed that the differences in the characteristic temperatures are negligible, since they lie within the range

Table 1
Properties of the fired glaze coatings (1100 °C)

Ref.	L* (±0.04)	a* (±0.02)	b* (±0.03)	Ib (±0.07)	Gloss (‰)	Ra (nm)
T	95.68	−0.23	0.36	93.3	48.3 ± 1.0	87 ± 30
TP05	95.28	−0.12	0.80	91.5	83.4 ± 0.5	28 ± 9
TP1	95.41	−0.18	1.04	90.9	85.9 ± 0.4	20 ± 4
TP2	94.82	−0.18	1.32	89.3	90.2 ± 0.3	15 ± 3
TP3	94.53	−0.26	1.92	87.2	88.1 ± 0.2	16 ± 4

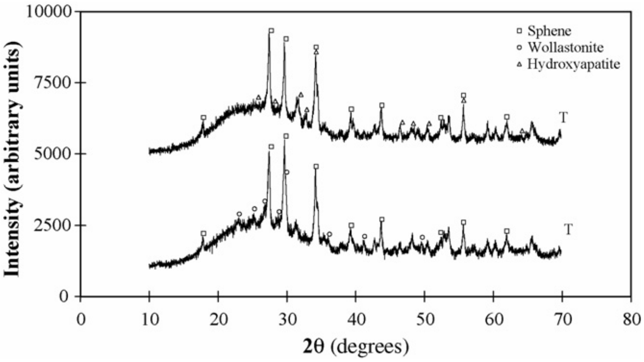

Fig. 1. XRD pattern of glazes T and TP1 heat treated at 1100 °C.

of error of the determinations. Consequently, the difference in surface roughness of these two glazes must be due to microstructural differences, i.e. differences in the quantity or type of crystalline phases present. The tests set out below were therefore conducted.

3.2. *Effect of the P_2O_5 addition on glaze microstructure*

In order to establish the effect of the P_2O_5 addition to frit T, we determined the crystalline phases present in the glazes at 1100 °C by XRD, with observation and analysis of the glaze surface by SEM.

Fig. 1 shows the results of the XRD determination of the phases present in glazes T and TP1. Glaze T displays two major crystalline phases, titanite (sphene) and wollastonite, whereas glaze TP1 contains sphene as major phase, together with traces of hydroxyapatite. Figs. 2–5 show SEM photographs of the glaze surfaces. At lower magnifications (Figs. 2 and 3), glaze T displays crystalline phases that are larger in size and are distributed less uniformly than those in glaze TP1. Observation and analysis at higher magnifications (Figs. 4 and 5) show that glaze T contains two types of crystals: those referenced W (corresponding to wollastonite), and those referenced S (corresponding to sphene). However, glaze TP1, which contains P_2O_5, only exhibits one crystalline phase, sphene (S), in addition to regions with a phase separation (PS).

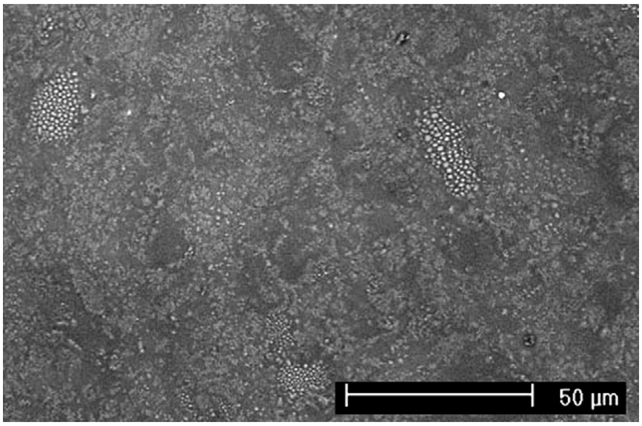

Fig. 3. SEM photograph of glaze TP1 surface (1100 °C).

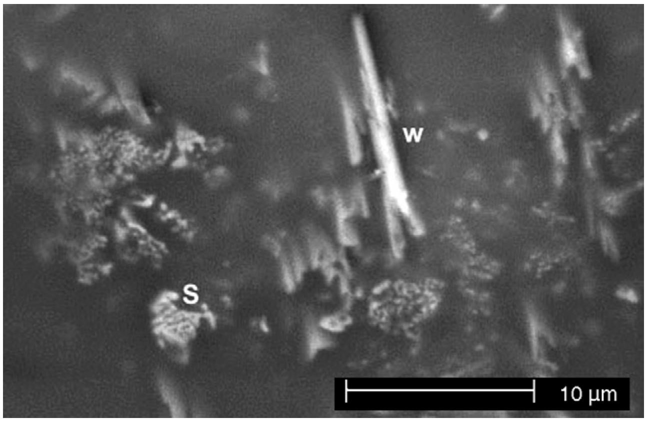

Fig. 4. SEM photograph of glaze T surface (1100 °C) higher magnifications.

These results show that gloss increases when P_2O_5 is introduced into the frit because the crystalline phases that evolve during tile firing are smaller in size. This is because P_2O_5 inhibits the formation of wollastonite, which devitrifies with larger crystals than sphene.

Figs. 6 and 7 show SEM photographs of glaze T and TP1 cross sections. Glaze T contains acicular and square crystals of wollastonite (W), small sphene crystals (SS), and irregularly shaped larger-size sphene crystals (LS). As also observed previ-

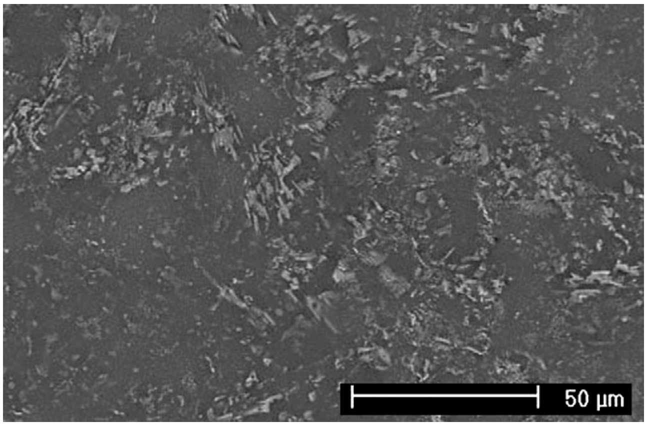

Fig. 2. SEM photograph of glaze T surface (1100 °C).

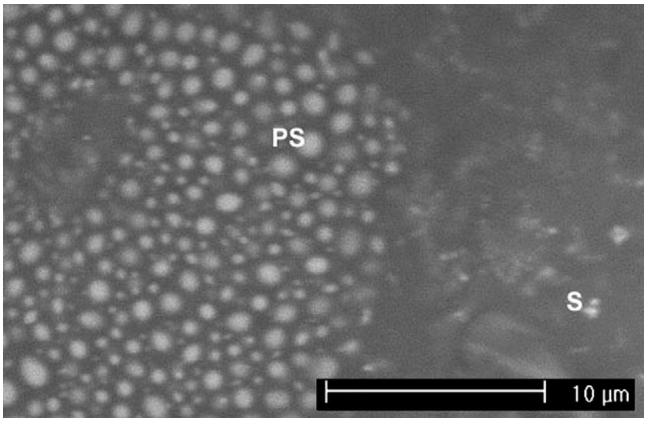

Fig. 5. SEM photograph of glaze TP1 surface (1100 °C) higher magnifications.

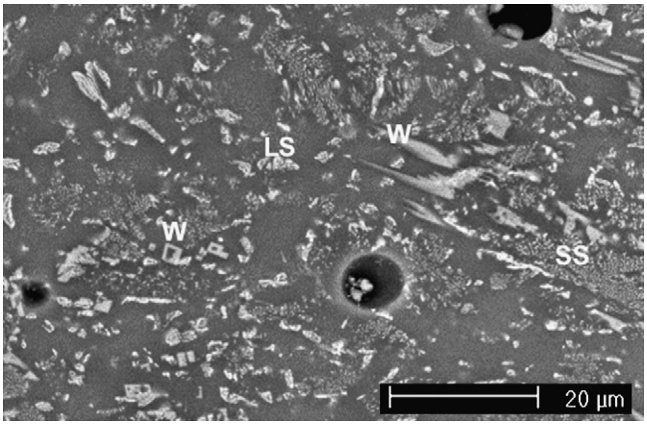

Fig. 6. SEM photograph of glaze T cross section (1100 °C).

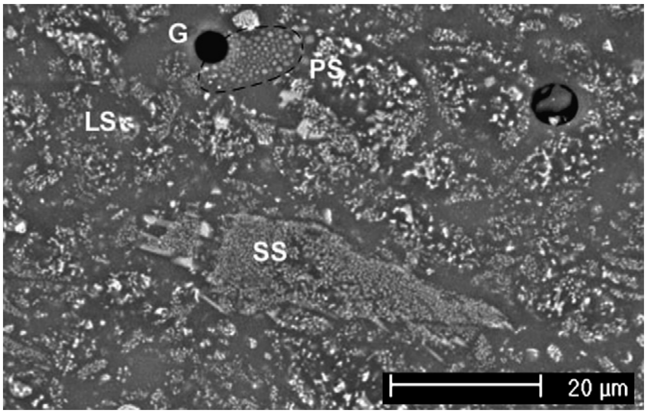

Fig. 7. SEM photograph of glaze TP1 cross section (1100 °C).

ously at the proper surface, the glaze TP1 cross section displays no wollastonite crystals, while the sphene crystals are generally smaller and more homogenously distributed. This glaze also evidences a phase separation (PS). The phosphorus that has been introduced is mainly found next to the sphene, and in the regions where phase separation has occurred: EDX analysis detected no phosphorus in the glassy phase (G).

The glaze cross sections were etched with hydrofluoric acid. Subsequent observation of these cross sections (Figs. 8 and 9) showed that in glaze T all the wollastonite crystals had dissolved, while in glaze TP1 the calcium-rich separated phase had dissolved.

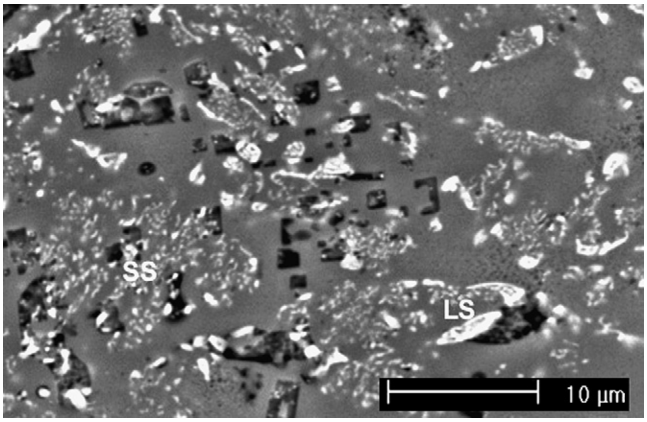

Fig. 8. Glaze T cross section after etching (1100 °C).

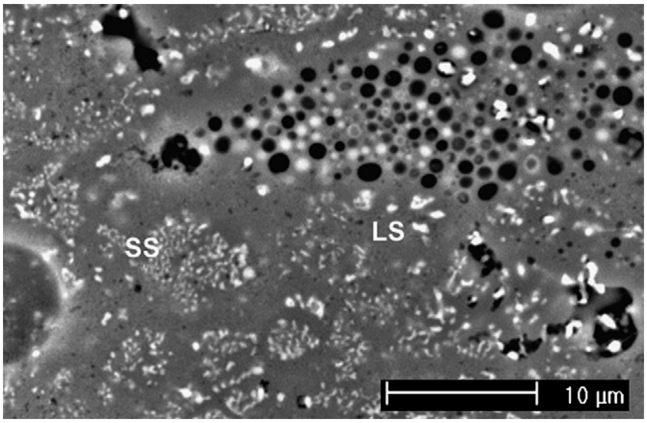

Fig. 9. Glaze TP1 cross section after etching (1100 °C).

These results confirm the observations of the glaze proper surfaces: the introduction of P_2O_5 inhibits wollastonite formation and yields glazes with smaller sphene crystals, distributed more homogeneously throughout the glaze. Furthermore, P_2O_5 also causes phases containing appreciable quantities of calcium to separate, which dissolve under acid attack.

3.3. Role of P_2O_5 in crystalline phase evolution

In order to determine the range of temperatures in which the crystalline phases devitrified, DTA was conducted on powder samples of glazes T and TP1. The results are shown in Fig. 10. Both samples exhibit exothermic bands (assignable to the devitrification processes), starting at the temperature at which glassy phase starts to form (T_{IC} of the fusion test, 830 °C).

Glaze T exhibits a wide exothermic band without any defined peaks, whereas glaze TP1 displays a well-defined exothermic peak around 950 °C. These results indicate that the P_2O_5 addition to the frit influences the crystallisation process. Figs. 11 and 12 show the results of the determination of the crystalline phases present in each glaze at different temperatures.

In glaze T (Fig. 11), the first phase to appear is wollastonite. The wollastonite content maximises around 900 °C and then dissolves progressively, until it almost disappears at 1200 °C.

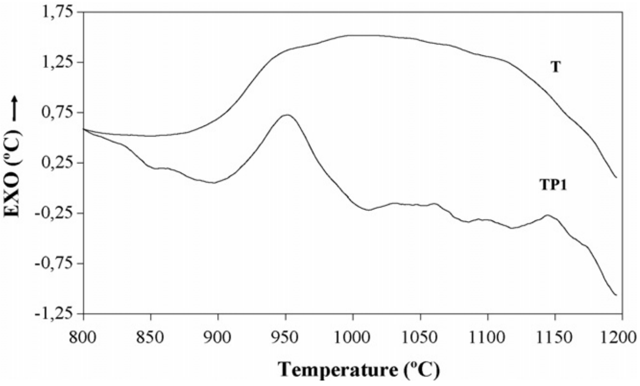

Fig. 10. DTA curves of glazes T and TP1.

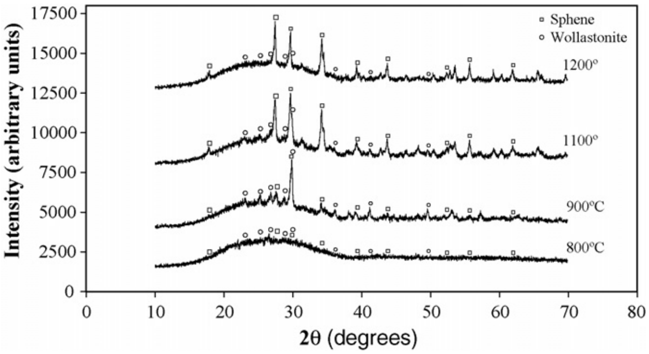

Fig. 11. XRD pattern of glaze T heat treated at different temperatures.

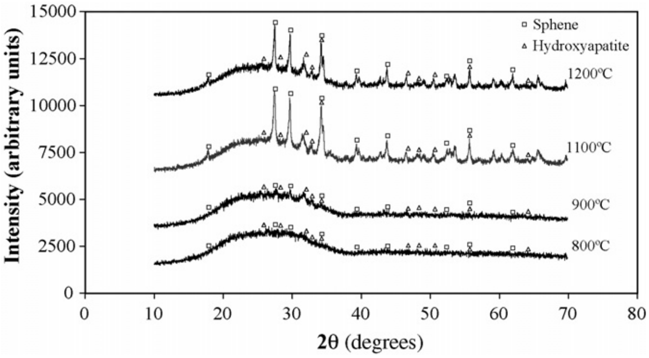

Fig. 12. XRD pattern of glaze TP1 heat treated at different temperatures.

A very small quantity of sphene has formed at 900 °C. The sphene content maximises at 1100 °C and decreases slightly at 1200 °C. In glaze TP1 (Fig. 12), hydroxyapatite forms first, followed by sphene, without any wollastonite appearing at all. Sphene behaviour at the highest temperatures is very similar to that observed in glaze T: the sphene content maximises at 1100 °C and decreases slightly at 1200 °C. The same tendency is observed for hydroxyapatite.

To verify these results, we fired glazes T and TP1 at different peak temperatures for further SEM observation. We chose three peak temperatures (1000, 1100 and 1200 °C) above the glaze shrinkage end temperature, since the glaze is porous at lower temperatures. Figs. 13–18 show details of the photographs taken during the SEM observation of these glaze cross sections.

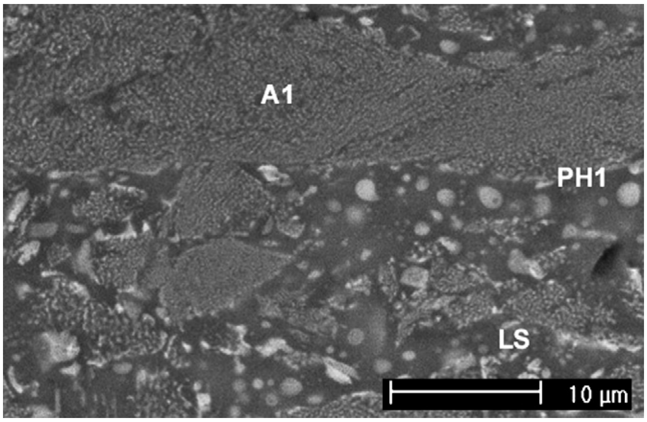

Fig. 13. SEM photograph of glaze T cross section (1000 °C).

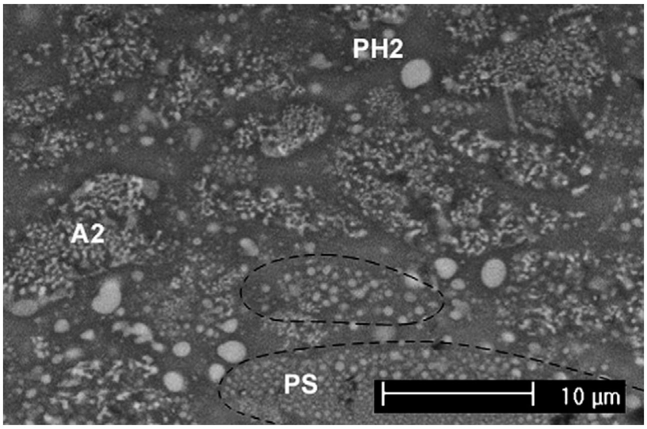

Fig. 14. SEM photograph of glaze TP1 cross section (1000 °C).

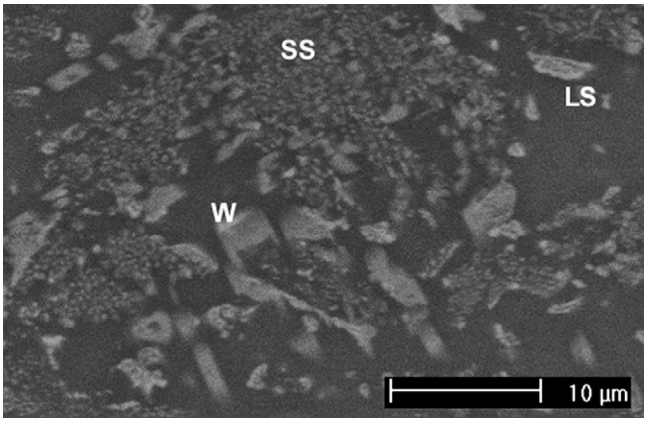

Fig. 15. SEM photograph of glaze T cross section (1100 °C) higher magnifications.

At 1000 °C (Figs. 13 and 14) both glazes exhibit a phase with a rounded shape (PH), the main difference being that in glaze T this phase corresponds to wollastonite (PH1), whereas in glaze TP1 this phase (PH2) contains important quantities of calcium and titanium, without reaching the ratio of sphene. Both glazes display regions with small crystals: analysis shows that in glaze T this region has an intermediate composition between wollastonite and sphene (A1), whereas in glaze TP1 the composition corresponds to sphene (A2), thus allowing the assumption that

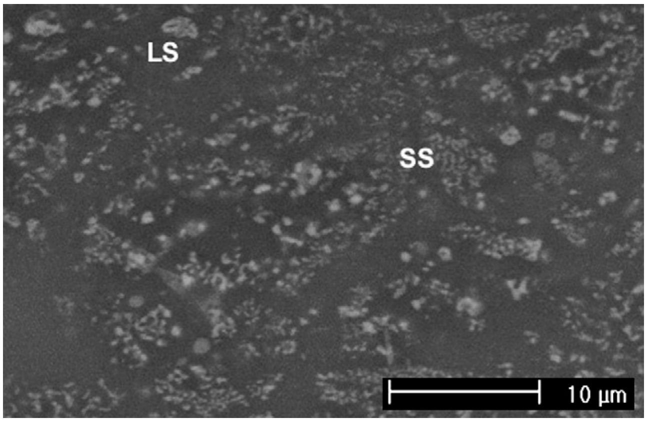

Fig. 16. SEM photograph of glaze TP1 cross section (1100 °C) higher magnifications.

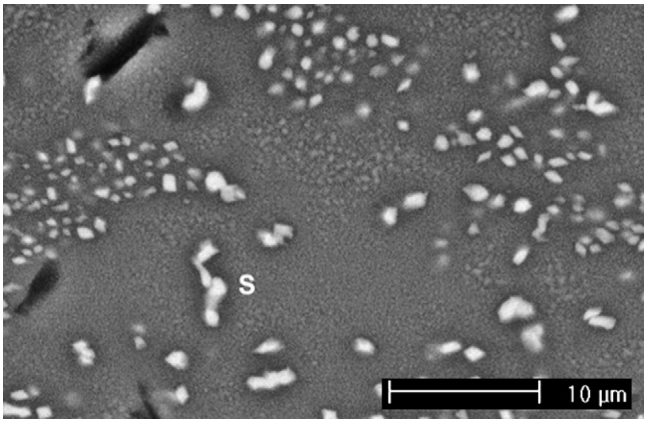

Fig. 17. SEM photograph of glaze T cross section (1100 °C).

sphene crystals are involved. Glaze T exhibits large sphene crystals (LS) which do not appear in glaze TP1. Finally, glaze TP1 displays areas with glassy-phase separation (PS), whose composition is similar to that of phase PH2 (important quantities of calcium and titanium).

The glazes fired at 1100 °C (Figs. 15 and 16) have already been discussed. These photographs were taken at higher magnification. They show that glaze T contains wollastonite crystals stemming from the evolution of phase PH1, observed at 1000 °C. This glaze also exhibits sphene crystals in two different sizes: the larger sphene crystals (LS) correspond to those that had formed at 1000 °C, whereas the smaller sphene crystals (SS) have evolved from the phases present in region A1 at 1000 °C. Glaze TP1 only exhibits sphene crystals, which are also in two sizes: the larger sphene crystals probably come from the evolution of phase PH2, while the smaller ones correspond to those already observed at 1000 °C in region A2.

At 1200 °C (Figs. 17 and 18) both glazes exhibit a similar appearance. In glaze T wollastonite has disappeared, dissolving in the arising glassy phase, while the sphene crystals (S) have grown. In glaze TP1 the sphene crystals (S) have also grown.

These results indicate that in this type of glaze P_2O_5 gives rise to a phase separation that favours devitrification of smaller sized sphene crystals and inhibits the formation of wollastonite crystals. These results are consistent with those reported elsewhere,[11,12] which indicate that introducing P_2O_5 into the composition of certain oxide systems like the one in the present study, which yield glass–ceramic materials, can favour obtaining microstructures with smaller crystals, because of the arising glassy phase separation which affects the development of the crystallisation process.

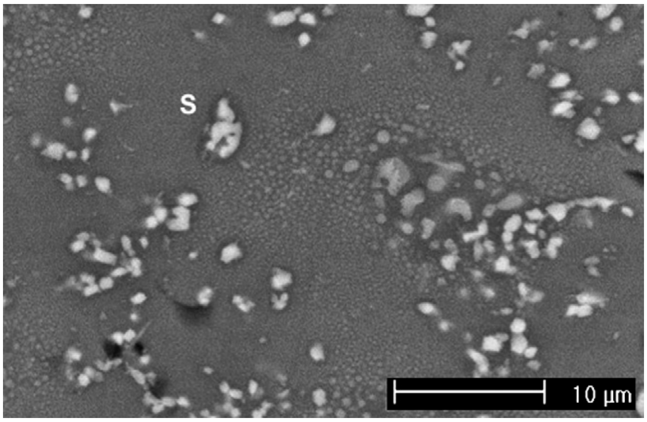

Fig. 18. SEM photograph of glaze TP1 cross section (1100 °C).

4. Conclusions

The present study has verified that introducing P_2O_5 into the studied type of frit, based on the system SiO_2-Al_2O_3-B_2O_3-CaO-K_2O-TiO_2, raises glaze gloss and yields glossy glazes with characteristics similar to those obtained in glazes opacified by zircon devitrification from frits that contain ZrO_2. The addition of 1% P_2O_5 by weight produces a glossy opaque white wall tile glaze with appropriate characteristics.

The characterisation of the starting glaze (T) and of this glaze composition with a 1 wt% P_2O_5 addition (TP1) has shown that P_2O_5 inhibits the formation of wollastonite, a crystalline species which devitrifies in the form of large crystals that reduce glaze gloss owing to the rise in surface roughness.

The study of the evolution of the crystalline phases in the studied glazes, with and without P_2O_5, has enabled determining how P_2O_5 acts. The study shows that P_2O_5 gives rise to a separation of small-size phases (droplets), which inhibits wollastonite formation, while concurrently favouring the formation of small-size sphene crystals. The effect of P_2O_5 disappears at high firing temperatures.

References

1. Escardino, A., Moreno, A., Amorós, J. L., Gozalbo, A., Aparici, J. and Sánchez, L. F., Study of crystalline-phase formation in white zirconium glazes. *Ceram. Acta*, 1996, **8**(6), 21–34.
2. Amorós, J. L., Escardino, A., Orts, M. J. and Moreno, A., Zirconium glazes used in fast single fired wall tile manufacture. Part 1. Crystallisation mechanism. *Br. Ceram. Trans.*, 1994, **93**(6), 224–228.
3. Escardino, A., Moreno, A., Amorós, J. L., Orts, M. J. and Barba, A., Zirconium glazes used in fast single fired wall tile manufacture. Part 2. Empirical model for fitting experimental data from devitrification process. *Br. Ceram. Trans.*, 2000, **99**(2), 72–76.
4. Zircon market tightens: driven by pre-cautionary buying or buoyant demand? Miner. Sands Rep., 2000, (November), 5–7.
5. Pearson, K., Grinding and bearing it: a zircon market insight. *Ind. Miner.*, 1999, **380**, 25–35.
6. Taylor, L., Zircon in ceramics: a price perspective. *Ind. Miner.*, 2001, **409**, 69–73.
7. O'Driscoll, M., The miller's tale: between a rock and a hard place. *Ind. Miner.*, 2003, **434**, 50–56.
8. Vincenzini, P., Biffi, G. and Ortelli, G., TiO_2 as an opacifier of ceramic glazes firing in the range 900–1000°C. *Ceramurgia*, 1975, **5**(1), 3–12.
9. Chen, G. K. and Liu, H. S., FTIR, DTA and XRD study of sphene ($CaTiSiO_5$) crystallization in a ceramic frit and a non-borate base glass. *J. Mater. Sci.*, 1994, **29**, 2921–2930.
10. Escardino, A., Moreno, A., Bou, E., Ibáñez, M. J., Muñoz, A. and Barba, A., Efecto del P_2O_5 sobre las propiedades superficiales de vidriados opacos con TiO_2. In *XLIV Congreso anual de la Sociedad Española de Cerámica y Vidrio*, 2004.
11. Moreno, A., Escardino, A., Bou, E. and Orts, M. J., Efecto del P_2O_5 en vidriados opacos por desvitrificación de circón. In *VIII Congreso Nacional de Materiales*, 2004, pp. 117–124.
12. McMillan, P. W., *Glass-ceramics* (*2nd ed.*). Academic Press, London, 1979, p. 43–47, 76, 104.